A simple, inexpensive photoelastic modulator

Kyle J. Braun, Christian R. Lytle, James A. Kavanaugh, James A. Thielen,[a] and Adam S. Green[b]
Department of Physics, University of St. Thomas, St. Paul, Minnesota 55105

(Received 24 March 2008; accepted 14 August 2008)

A block of birefringent gelatin acts as a variable retarder when driven harmonically by a speaker coil and can be used to vary the polarization of a laser beam sinusoidally. We model this effect with Mueller matrices and show that the gelatin behaves much like a commercial photoelastic modulator and is suitable for a variety of polarimetry experiments in an advanced undergraduate optics course. © *2009 American Association of Physics Teachers.*
[DOI: 10.1119/1.2978001]

I. INTRODUCTION

Photoelastic modulators utilize stress-induced birefringence to continuously vary the polarization of light and have been widely used since the 1960s[1–4] in research and industrial applications that require very precise polarimetry. Because they consume little power and have large apertures, acceptance angles, and retardance ranges for a broad spectral region,[1–6] photoelastic modulators are extremely versatile.[6]

Photoelastic modulators are also excellent pedagogical tools for students in a junior or senior level optics course. We have used a commercial photoelastic modulator (Hinds Instruments PEM-90) to introduce our students to advanced topics in polarimetry after teaching them about Jones and Mueller polarization matrices. Commercial instruments cost thousands of dollars, so it is not feasible for us to outfit each station in our teaching laboratory with its own photoelastic modulator. We generally prefer to have our students perform identical experiments simultaneously rather than rotate through unrelated lab stations, so we decided to build several inexpensive photoelastic modulators from off-the-shelf materials.

After testing stiff birefringent plastics such as polycarbonate which requires inconvenient magnitudes of stress, we searched for a material with a lower elastic modulus and more easily manipulated birefringence. Ferguson's article[7] about polarized light demonstrations inspired us to try gelatin as the optical element of a simple photoelastic modulator. We found that it works surprisingly well when placed in a plastic mold and driven harmonically by a speaker coil. In the following we describe the design and operation of the gelatin photoelastic modulator and suggest applications suitable for advanced students.

II. CONSTRUCTION AND OPERATION OF A PHOTOELASTIC MODULATOR

In a commercial photoelastic modulator a piezoelectric transducer mechanically compresses and stretches an optical element sinusoidally and makes it act as a variable wave plate with a retardance of $\Delta(t)=\Delta_0 \sin(\omega t)$, where Δ_0 is the retardance amplitude and $\omega/2\pi$ is the driving frequency f. This frequency is usually set to match that of a natural acoustic resonance in the optical element and minimizes driving power requirements. Most photoelastic modulators operate at a fixed frequency, typically in the 20–100 kHz range for commonly used optical materials like fused silica, LiF, CaF_2, ZnSe, and Si.[5] The gelatin photoelastic modulator operates on a similar principle, but has some design differences that lead to a slightly different pattern of retardance modulation.

We use Knox® gelatine and prepare it according to the directions on the package, adding only water to the powder and stirring gently to avoid bubble formation. We pour it slowly into a 2 in. × 1.5 in. × 0.75 in. Delrin® mold that has two removable sides to allow solidified gelatin to expand slightly when compressed (see Fig. 1). (Gelatin does not perform well as a photoelastic modulator if it cannot freely expand along one axis.) To prevent the gelatin from sticking to the removable sides, we coat these sides with cooking spray.

The front and back of the mold contain two 0.5 in. × 1.5 in. slots over which microscope slides are glued to serve as optical windows. The slides help maintain a stable laser beam position by preventing the optical surfaces of compressed gelatin from deforming and have a negligible effect on the polarization states of normally incident light. During refrigeration the top of the mold is covered with a rigid, transparent piece of plastic that lightly touches the surface of the liquid gelatin. The plastic prohibits the formation of a meniscus that would later prevent us from applying uniform pressure to the solidified gelatin. The plastic's transparency allows us to see if unwanted bubbles are trapped on the gelatin's surface. This cover is coated with cooking spray for easy removal.

To make the gelatin block act as a photoelastic modulator we compress it sinusoidally with a flat, transparent piece of plastic attached to the tip of a PASCO mechanical wave driver (model SF-9324), which is controlled by a standard function generator. The frequency and amplitude ranges (0–5 kHz and 0–7 mm *p-p*, respectively) of this robust speaker coil match the elastic properties of gelatin quite well for our applications. The driver hangs upside down from a post and pushes downward on the gelatin (see Fig. 1). The transparency of the plastic compressor allows us to observe if it makes uniform contact with the gelatin's surface. If the applied pressure is not uniform, the stress-induced birefringence and the resulting polarization modulation will not be symmetric. We control the amount of contact between the two surfaces by adjusting the vertical position of a small lab jack placed beneath the Delrin housing. A stable lab jack permits us to coarsely adjust the average level of stress birefringence, and an adjustable dc offset voltage from the function generator allows for fine tuning of this parameter. [An *x-y* stage mounted at the base of the lab jack is sometimes useful for optimizing stress uniformity (not shown in Fig. 1.)]

Because we apply compressive stress but no tensile stress

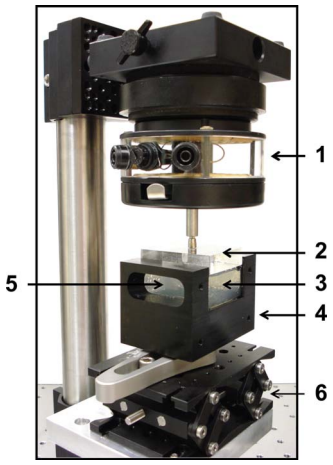

Fig. 1. Gelatin photoelastic modulator apparatus. (1) PASCO wave driver, (2) plastic compressor, (3) gelatin block, (4) Delrin mold with removable sides, (5) one of two microscope slides as an optical window, and (6) lab jack.

to the gelatin, the retardance does not oscillate about zero as it does for a Hinds PEM-90. It instead oscillates about an offset level of our choosing

$$\Delta(t) = \Delta_0 \sin(\omega t) + \Delta_{\text{offset}}. \tag{1}$$

This feature is convenient because some applications incorporate a quarter-wave plate in conjunction with a commercial photoelastic modulator to achieve different ranges of output polarization states. Our photoelastic modulator does not require the additional wave plate because we can choose a quarter-wave (or other) offset retardance by adjusting both the vertical position of the gelatin and the dc offset voltage of the drive signal. If Δ_{offset} equals an even multiple of π (half-wave retardance), our photoelastic modulator effectively operates in the same fashion as a Hinds PEM-90.

Our gelatin blocks work best when modulated in the frequency range of 25–40 Hz. We usually have to fine-tune the frequency to two decimal places when searching for the resonance that produces sinusoidal birefringence with the largest amplitude. A function generator with a 0–10 $V_{p\text{-}p}$ output is sufficient for achieving up to a full wave of retardance. A quarter wave typically corresponds to 1.5–2.5 $V_{p\text{-}p}$, and a half wave is achieved by doubling this voltage.

To find the best resonance and calibrate the device we place it between crossed linear polarizers oriented at ± 45 from its fast axis (Fig. 2), which is along the vertical direction of the applied force on the gelatin. We use a photodetector connected to an oscilloscope to monitor the polarization-dependent transmitted intensity of a laser beam.

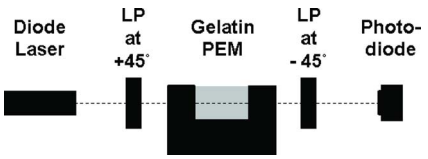

Fig. 2. Setup for calibration of the gelatin photoelastic modulator. The latter is placed between crossed linear polarizers which are oriented at ±45° from the modulator's fast axis (vertical direction). The time-dependent transmitted intensity of a laser beam is monitored by a photodiode connected to an oscilloscope.

Although commercial photoelastic modulators often require detectors with bandwidths well above 100 kHz,[8] nearly any inexpensive detector will suffice for our photoelastic modulator because of its low modulation frequency. We place a laser line filter and an iris diaphragm over the detector to reduce pickup from room lights, which can otherwise be problematic at these frequencies.

By using the theoretical waveforms described in Sec. III as a guide, we can accurately determine if the photoelastic modulator produces the desired values of retardance. When the photoelastic modulator's retardance magnitude is a multiple of a quarter wave, calibration can be performed by observing wave forms on the oscilloscope because they are symmetric and easy to interpret. The wave forms are often more complicated when the photoelastic modulator is used to measure the birefringence or dichroism of an optical target. In such cases it is customary to process the photoelastic modulator signals with either lock-in amplifiers (as described in Sec. IV) or fast Fourier analysis of digitized wave forms.[9] We have successfully used both methods in our experiments. When using the latter method, we capture wave forms with either a computer-interfaced digital oscilloscope or an analog input of a data acquisition board, and then we use LabVIEW's fast Fourier transform method to measure the voltage amplitudes of photoelastic modulator driving frequency harmonics. We also extract the dc component, which is a measure of the time averaged total light throughput. Some applications require ac harmonics to be normalized to this dc signal, and others utilize the ratio of two ac harmonics. (For further information about signal detection and processing with commercial photoelastic modulators, see Refs. 9 and 10.)

In summary, the gelatin photoelastic modulator in Fig. 1 cost only one box of gelatin because all other components were already in our optics laboratory. If the basic parts were purchased, a gelatin photoelastic modulator would cost about $300–650 (in contrast to the Hinds PEM-90 and its driver which cost $5000 in 2004). This price tag for the gelatin apparatus does not include a function generator, oscilloscope, computer interface board, and mounting hardware because they are ubiquitous in physics labs. A 3 in. × 3 in. × 12 in. block of Delrin can be shipped from McMaster–Carr for about $95. Because only a 3 in. cube is needed for our design, a single gelatin photoelastic modulator housing costs only about $24. The wave driver currently sells for $214.[11] Lab jacks vary greatly in price: the Thorlabs Mini Lab Jack (model L200) cost $390, but Edmund Scientific sells an Economy Lab Jack (#3108200) for only $65.

III. CALIBRATION OF THE PHOTOELASTIC MODULATOR

We use Mueller matrices and Stokes vectors to analyze the operation and application of our photoelastic modulator. Thorough discussions of the Mueller–Stokes formalism can be found in numerous places.[12–14] In brief, the Stokes vector is a column vector $S=(S_0,S_1,S_2,S_3)$ in which S_0 represents the total light intensity, S_1 indicates the relative contributions of horizontal linear polarization (HLP) and vertical linear polarization (VLP), S_2 refers to linear polarization at +45° (LP+45) and linear polarization at −45° (LP−45), and S_3 is a measure of the right- and left circular polarization compo-

nents (RCP and LCP). Stokes vectors are acted on by 4×4 Mueller matrices M which represent optical elements in the beam path: $S_{\text{out}}=M_{\text{element}}S_{\text{in}}$.

The Mueller matrix M_{PEM} of the gelatin photoelastic modulator can be obtained from the matrix for a general linear retarder with retardance δ and fast axis angle θ measured from the horizontal[13]

$$M_{\text{ret}}=\begin{pmatrix}1 & 0 & 0 & 0\\ 0 & C_{2\theta}^2+S_{2\theta}^2C_\delta & S_{2\theta}C_{2\theta}(1-C_\delta) & -S_{2\theta}S_\delta\\ 0 & S_{2\theta}C_{2\theta}(1-C_\delta) & S_{2\theta}^2+C_{2\theta}^2C_\delta & C_{2\theta}S_\delta\\ 0 & S_{2\theta}S_\delta & -C_{2\theta}S_\delta & C_\delta\end{pmatrix}, \tag{2}$$

where $C_{2\theta}^2=\cos^2 2\theta$, $S_{2\theta}^2=\sin^2 2\theta$, $C_\delta=\cos\delta$, and $S_\delta=\sin\delta$. In our case $\theta=90°$ and $\delta=\Delta(t)$ from Eq. (1). Therefore,

$$M_{\text{PEM}}=\begin{pmatrix}1 & 0 & 0 & 0\\ 0 & 1 & 0 & 0\\ 0 & 0 & \cos\Delta(t) & -\sin\Delta(t)\\ 0 & 0 & \sin\Delta(t) & \cos\Delta(t)\end{pmatrix}. \tag{3}$$

When a linear polarizer at 45° is placed in front of the photoelastic modulator, the Stokes vector S_{PEM} for light exiting the photoelastic modulator is

$$S_{\text{PEM}}=M_{\text{PEM}}S_{\text{LP+45}}=M_{\text{PEM}}\begin{pmatrix}1\\0\\1\\0\end{pmatrix}=\begin{pmatrix}1\\0\\\cos\Delta(t)\\\sin\Delta(t)\end{pmatrix}. \tag{4}$$

This vector shows how the output polarization state continuously varies among the linear, elliptical, and circular states. If an analyzer oriented at −45° with a Mueller matrix of

$$M_{\text{LP-45}}=\frac{1}{2}\begin{pmatrix}1 & 0 & -1 & 0\\ 0 & 0 & 0 & 0\\ -1 & 0 & 1 & 0\\ 0 & 0 & 0 & 0\end{pmatrix} \tag{5}$$

is placed after the photoelastic modulator, the output polarization state seen by a downstream detector is

$$S_{\text{out}}=M_{\text{LP-45}}S_{\text{PEM}}=\frac{1}{2}[1-\cos\Delta(t)]\begin{pmatrix}1\\0\\-1\\0\end{pmatrix}, \tag{6}$$

which reveals that the detector measures a time-varying intensity of

$$I(t)=\frac{1}{2}[1-\cos\Delta(t)]. \tag{7}$$

We use Eq. (7) to calibrate the photoelastic modulator when it is placed in the configuration shown in Fig. 2.

Figure 3(a) shows theoretical plots of the photoelastic modulator retardance $\Delta(t)$ [Eq. (1)] for one period of oscillation. Curves 1–3 correspond to the retardance amplitudes $\Delta_0=\pi/2$, π, and $3\pi/2$ rad (quarter-, half-, and three-quarters-wave retardances), respectively, and for Δ_{offset} equaling an even multiple of π. Figure 3(b) shows theoretical curves of $I(t)$ [Eq. (7)] at the photodetector for the same

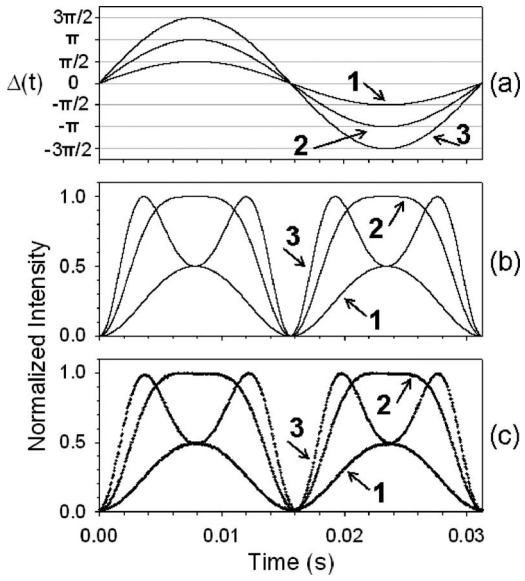

Fig. 3. Calibration of the photoelastic modulator between crossed polarizers for effectively zero retardance offset: $\Delta_{\text{offset}}=2n\pi$ $(n=1,2,3,\ldots)$. (a) Theoretical retardance variation at the driving frequency f for (1) $\Delta_0=\pi/2$, (2) $\Delta_0=\pi$, and (3) $\Delta_0=3\pi/2$. (b) Theoretical curves of the transmitted $I(t)$ for these same retardance amplitudes. (c) Corresponding plots of the experimental data. The curves are normalized to unit intensity.

retardance settings. The two intensity peaks in curve 1 of Fig. 3(b) occur where the photoelastic modulator's quarter-wave retardation converts the LP+45 input state into circularly polarized light, for which half the intensity passes the second polarizer. The full-intensity peaks of curve 2 result from the photoelastic modulator acting as a half-wave plate which rotates the incident LP+45 light by 90° to align it with the second polarizer's transmission axis. In curve 3 peaks again occur when the retardance is half- wave, and the half-maximum intensities occur when the retardance is a three-quarters wave because it produces circular polarization.

Figure 3(c) contains data captured by an oscilloscope and demonstrates that the gelatin photoelastic modulator is capable of producing the correct wave forms for each of the retardance amplitudes we considered. To obtain these curves we adjusted the function generator's voltage amplitude until the oscilloscope signal closely resembled the theoretical predictions. Doing so by eye is sufficient to achieve about 1%–2% accuracy, especially for half-wave retardance because the curve peaks remain flat for only a small range of voltages. Using the averaging function of a digital oscilloscope improves the accuracy.

Figure 4 shows the predictions and results for a quarter-wave offset retardance ($\Delta_{\text{offset}}=\pi/2$). These curves can be obtained by placing a quarter-wave plate after the photoelastic modulator (with its fast axis aligned with the photoelastic modulator's) or by adjusting the dc component of the applied stress with the lab jack and function generator. In this example we used the latter method to show that it works equally well. Curves 1 and 2 of the top graph show $\Delta(t)$ for $\Delta_0=\pi/2$ and π, and curves 1 and 2 of the middle graph show the resulting $I(t)$ for these retardances. The flat peak of $I(t)$ in curve 1 occurs when the photoelastic modulator's half-wave retardance rotates the input LP+45 state by 90°, and the flat trough at zero transmission corresponds to zero effective photoelastic modulator retardance. In curve 2 of the middle

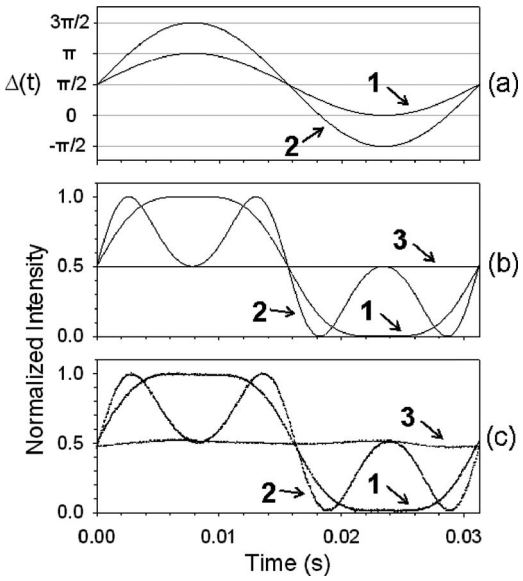

Fig. 4. Calibration of the photoelastic modulator between crossed polarizers for quarter-wave offset retardance: $\Delta_{\text{offset}}=n\pi/2$ $(n=1,5,7,\ldots)$. (a) Theoretical plot of $\Delta(t)$ for (1) $\Delta_0=\pi/2$ and (2) $\Delta_0=\pi$. (b) Curves 1 and 2 are theoretical predictions of the transmitted $I(t)$ for the same retardance amplitudes. Curve 3 indicates that half intensity should always be transmitted when the input linear polarization is oriented along the photoelastic modulator's fast axis. (c) Experimental data for the same three conditions used in (b).

graph $I(t)$ has maxima and minima when the retardance is half wave or zero and reaches only half its maximum when the photoelastic modulator produces opposite circular polarizations at the extreme values of its retardance modulation. The experimental curves 1 and 2 in the bottom graph reveal that the gelatin photoelastic modulator again behaves as predicted.

Curve 3 in Fig. 4 shows that the intensity should ideally remain constant at half its maximum value when the input linear polarizer is aligned with the photoelastic modulator's slow or fast axes, regardless of the photoelastic modulator's retardance amplitude and offset. This state should encounter only one refractive index, so no relative phase shift should occur. Experimental curve 3 in the bottom graph demonstrates that a slight intensity modulation is sometimes still present even after careful alignment of the wave driver and optical components. Although the gelatin's birefringence is not always perfectly symmetric, the homemade photoelastic modulator still works well for applications that do not require high precision.

Many experiments, including the one described in Sec. IV, can be performed with quarter-wave retardance amplitude and effectively zero offset retardance ($\Delta_0=\pi/2$ and $\Delta_{\text{offset}}=0$, as in Fig. 3, curve 1). For optimal calibration of this configuration we first set the photoelastic modulator to half-wave retardance ($\Delta_0=\pi$) by visually matching the oscilloscope's wave form to Fig. 3, curve 2. The flat peaks allow us to carefully determine the maximum transmitted intensity $I_{\max}$. When we halve the driving voltage amplitude to obtain quarter-wave retardance, the wave form should peak at $I_{\max}/2$. Sometimes this voltage change causes the wave form to become slightly asymmetric or fall short of $I_{\max}/2$, so we adjust the driving voltage amplitude and offset the alignment of the entire photoelastic modulator apparatus, and/or the orientation of the input polarizer. We also make sure that the laser beam passes through the center of the gelatin block and enters it at normal incidence. Once the wave form appears to be correct, we rotate the downstream linear polarizer back and forth between −45° and +45°. If the photoelastic modulator correctly produces polarizations that range from RCP to LP+45 to LCP, we see a flat line at $I_{\max}/2$ when the analyzer is oriented at 0°. With the analyzer at +45° (parallel to the first polarizer), the waveform should be a vertical mirror image of Fig. 3, curve 1, with peaks at $I_{\max}$ and troughs at $I_{\max}/2$. If we do not see the correct wave forms, we again make the adjustments mentioned previously. Several iterations of these steps are normally required to achieve the desired signal.

Students typically require most of a lab period to set up and learn how to calibrate their photoelastic modulators in this fashion, assuming that they have worked through the theory and prepared the gelatin in advance. Calibration takes less time (perhaps half an hour) for experienced students.

IV. APPLICATIONS

Although the photoelastic modulator calibration procedure makes an instructive lab activity by itself, students can choose from a vast array of experiments that involve linear and circular birefringence or linear and circular dichroism. The research literature is full of ideas, and many articles provide sufficiently detailed calculations so that students can readily learn how to model their systems with Jones or Mueller matrices.[15] As an illustration, the following calculation demonstrates one way of using Mueller matrix theory in conjunction with harmonic detection to measure the retardance of a wave plate. This type of experiment is a good starting place for students because it is relatively straightforward.

If the gelatin photoelastic modulator is calibrated when placed between crossed linear polarizers (see Fig. 2), a wave plate can be inserted between the photoelastic modulator and the analyzer to give the Stokes vector at the location of the detector

$$S_{\text{out}} = M_{\text{LP}-45} M_{\text{ret}} M_{\text{PEM}} S_{\text{LP}+45}. \tag{8}$$

If we use the matrices in Eqs. (2)–(6), the S_0 parameter of this output vector gives the time-varying output intensity

$$I(t) = \frac{1}{2}[1 - (S_{2\theta}^2 + C_{2\theta}^2 C_\delta)\cos\Delta(t) - C_{2\theta} S_\delta \sin\Delta(t)]. \tag{9}$$

As mentioned in the context of Eq. (2), θ refers to a generic wave plate's fast axis orientation relative to the horizontal, and δ is the wave plate's retardance. As before, $\Delta(t)$ is the gelatin photoelastic modulator's retardance given by Eq. (1). To make Eq. (9) compatible with fast-Fourier transform and lock-in detection methods, $\cos\Delta(t)$ and $\sin\Delta(t)$ can be expanded into harmonic components using the Fourier–Bessel series

$$\cos[\Delta_0 \sin(\omega t)] = J_0(\Delta_0) + \sum_{2k} 2J_{2k}(\Delta_0)\cos[(2k)\omega t]$$

and

$$\sin[\Delta_0 \sin(\omega t)] = \sum_{2k+1} 2J_{k+1}(\Delta_0)\sin[(2k+1)\omega t], \tag{10}$$

where $J_n(x)$ is a order-n Bessel function of the first kind. We have let Δ_{offset} equal an even multiple of π, which is acceptable for our retardance measurements.

Because harmonics above $2f$ are not needed in most photoelastic modulator applications, the output intensity can be written as

$$I(t) = \frac{1}{2}[1 - (S_{2\theta}^2 + C_{2\theta}^2 C_\delta)(J_0(\Delta_0) + 2J_2(\Delta_0)\cos 2\omega t) - C_{2\theta} S_\delta (2J_1(\Delta_0)\sin \omega t)]. \quad (11)$$

If we group dc, $1f$, and $2f$ terms separately, we obtain

$$I(t) = I_{\mathrm{dc}} - I_{1f}\sin \omega t - I_{2f}\cos 2\omega t, \quad (12)$$

where

$$I_{\mathrm{dc}} = \frac{1}{2}[1 - (S_{2\theta}^2 + C_{2\theta}^2 C_\delta)J_0(\Delta_0)],$$

$$I_{1f} = C_{2\theta} S_\delta J_1(\Delta_0), \text{ and} \quad (13)$$

$$I_{2f} = (S_{2\theta}^2 + C_{2\theta}^2 C_\delta)J_2(\Delta_0).$$

Following Oakberg's suggestion,[16,17] the dc term can be ignored if the ratio of ac harmonics is considered

$$\frac{I_{1f}}{I_{2f}} = \frac{C_{2\theta} S_\delta J_1(\Delta_0)}{(S_{2\theta}^2 + C_{2\theta}^2 C_\delta)J_2(\Delta_0)}. \quad (14)$$

This ratio also allows us to disregard the intensity fluctuations of the light source as well as multiplicative experimental constants like gain settings on the photodetector. Therefore, if the detection system records voltage magnitudes V_{1f} and V_{2f} corresponding to intensities I_{1f} and I_{2f}, then $I_{1f}/I_{2f} = V_{1f}/V_{2f}$.

In Eq. (13) the $1f$ signal reaches its maximum magnitude when the retarder's fast axis is oriented horizontally or vertically. Hence, the voltage V_{1f} can be monitored for precise alignment of this axis. As the retarder's fast axis is rotated from the horizontal to the vertical, the change in sign of I_{1f} shows up as a 180° phase shift on a lock-in amplifier; this information is not needed for our retardance measurements and harmonic magnitudes are sufficient.

Fast axis orientations of $\theta = 0°$ and 90° simplify Eq. (14) and allow the wave plate's retardance to be expressed as

$$\delta = \tan^{-1}\left[\frac{V_{1f}}{V_{2f}} \cdot \frac{J_2(\Delta_0)}{J_1(\Delta_0)}\right]. \quad (15)$$

For this application we set the photoelastic modulator's retardance amplitude Δ_0 equal to $\pi/2$ to simplify the photoelastic modulator calibration using the oscilloscope (as described in Sec. III). At this amplitude the Bessel functions have the values $J_1(\pi/2) = 0.5668$ and $J_2(\pi/2) = 0.2497$. Corrections must be made to retardance measurements that exceed quarter wave because of the tangent function's ambiguous nature for those values. Such corrections might not be apparent when testing unknown wave plates at a single wavelength, but they are usually obvious for commercial plates and for variable wave plates that can be set to truly zero retardance.

Figure 5 shows our measurements of a half-wave plate designed for 780 nm. We used a 637.5 nm diode laser and tilted the wave plate first about its slow axis and then about its fast axis to show that it can be tuned to become a half- or three-quarters-wave plate at this wavelength. The dots on the graph represent data collected using the gelatin photoelastic modulator, and the solid curves represent data taken with a Hinds PEM-90 for comparison. The overlap of the two data sets demonstrates the consistency of the two modulators. Each point is the average of 100 lock-in amplifier measurements recorded at a rate of 10 Hz using LabVIEW. Statistical error bars are smaller than the dots on the graph. As expected,[18,19] the retardance increases approximately quadratically when tilting about the slow axis and decreases in a similar fashion when tilting about the fast axis.

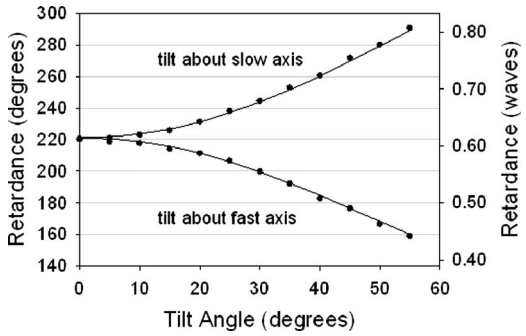

Fig. 5. Retardance versus tilt angle for a half-wave plate designed for 780 nm light. Retardance was measured using a 637.5 nm diode laser, and the plate was tilted away from normal incidence, first about its slow axis, and then about its fast axis. The solid curves represent data measured with a Hinds PEM-90, and dots denote data collected with the gelatin photoelastic modulator. The overlap of the data sets shows that the two PEMs produce consistent results.

At normal incidence the PEM-90 measured a retardance of $221.12° \pm 0.02°$ and the gelatin PEM measured $220.1° \pm 0.1°$. These small uncertainties are purely statistical. By comparison, published data[20] show that the Hinds PEM-90 can produce statistical errors below 0.002° if used in a variation of our optical configuration with electronic filtering and a different mathematical analysis. The larger error produced by the gelatin can result from the misalignment of the wave driver, temperature variations, and mechanical creep of the gelatin block. Sometimes retardances measured with the gelatin vary as much as a few degrees over several minutes. To reduce these effects the gelatin should be brought to room temperature after refrigeration, and the average value of the vertical stress and Δ_{offset} should be kept as small as possible (for example, $\Delta_{\mathrm{offset}} = \pi/2$ is preferable to $5\pi/2$, even though the two are functionally equivalent). The plastic compressor attached to the wave driver should be centered on the gelatin block and parallel to its top surface, and the laser beam should pass along the gelatin's centerline. Although our photoelastic modulator does not utilize feedback stabilization circuitry such as found in the PEM-90, we can usually obtain statistical uncertainties well below 1.0° by following these precautions. In a separate experiment with a different gelatin block, we compared the long-term stability of normal-incidence retardance measurements for the two photoelastic modulators. Figure 6 shows that the gelatin photoelastic modulator is stable to within about 0.23° *p-p* for this particularly good half-hour run, compared to 0.08° *p-p* for the PEM-90. Students more commonly achieve about 0.5°–1.0° *p-p* stability with their setups.

The 1.02° difference in mean retardance values measured by the two photoelastic modulators at normal incidence (Fig. 5) could be due to a non-uniform retardance across the wave plate's profile and a slightly inconsistent laser beam

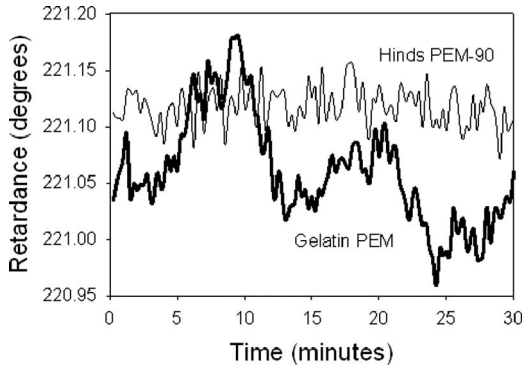

Fig. 6. Long-term stability of retardance measurements using the Hinds PEM-90 (light line) and the gelatin photoelastic modulator (bold line). The retarder is the same one referred to in Fig. 5, but data were taken at a later date with a different gelatin photoelastic modulator.

position, or even a slightly off-normal angle of incidence. It could also be due to calibration errors or drifting of the gelatin photoelastic modulator's retardance. Nevertheless, both experimental results are close to the following theoretical prediction. The retardance for wavelength λ introduced by a linear retarder with thickness t is $\delta=360°\ (n_e-n_o)t/\lambda$, where (n_e-n_o) is the linear birefringence (difference in refractive indices for extraordinary and ordinary linear polarization components). The manufacturer's claim of $\delta=180°$ at 780 nm leads to $(n_e-n_o)t=390$ nm. Therefore, the retardance should be approximately 220.2° at 637.5 nm for normally incident light. [A 180° correction was made to the ~40° retardance measured using Eq. (15).] We do not know the manufacturer's uncertainty for this particular wave plate's retardance; a retardation tolerance of $\pm\lambda/600$ to $\pm\lambda/200$ is typical for many wave plate manufacturers.[21] Thus, our wave plate's actual retardance probably lies within the $180° \pm 1.8°$ range for 780 nm light, which translates to $220.2° \pm 2.2°$ for our 637.5 nm laser.

In addition to linear birefringence experiments, students can measure the circular birefringence (optical activity) of chiral molecules in solution using a similar procedure. Our tests with glucose in water give the well-known linear increase in rotation angle with molecular concentration. We typically measure a minimum detectable rotation angle of about 0.2°, which is sufficient for many applications but far from the 0.001° achievable with the PEM-90.[22] Our lower limit is largely determined by the slightly asymmetric gelatin oscillation that we referred to in the context of Fig. 4.

Experiments with chirality can prompt discussions with students about biomedical applications of the photoelastic modulator such as the noninvasive detection of blood-glucose levels for diabetic patients. Photoelastic modulator systems can accurately measure small concentrations of chiral molecules in turbid media (latex microspheres in water), even when multiple scattering strongly depolarizes the incident laser beam.[6,23–25] Although a clinical glucometer based on polarimetry has not yet been realized, this area of research shows promise. If an avalanche photodiode or photomultiplier tube were available to detect diffusely scattered light, students could use their gelatin photoelastic modulators to learn about the systems described in Refs. 6 and 23–25. Many of these experiments could be performed with high enough sugar concentrations so that rotation angles remain well above the detection limit of 0.2°. We plan to have the students in our optics course examine these and other exciting topics in the near future.

V. CONCLUSIONS

We have demonstrated that a block of gelatin can serve as the optical element of a simple photoelastic modulator. The mold that supports the gelatin is easy to construct, and the PASCO wave driver we use to modulate the gelatin's birefringence is commonly found in physics labs. This system works well after the user has practiced aligning and calibrating it a few times, and it serves effectively as a pedagogical tool in the undergraduate optics laboratory.

The gelatin photoelastic modulator has three primary limitations. (1) The polarization signals it produces tend to drift if the precautions mentioned in Sec. IV are not taken. (2) Small asymmetries in its birefringence prohibit it from being used for high-precision experiments. (3) The gelatin block has a lifetime of 3–5 days, beyond which it becomes dehydrated from evaporation. The lifetime can be modestly extended by storing it in a refrigerated air-tight container. Alternately, ethylene glycol or a similarly stable solvent could be used as a substitute for water,[26] though we have not yet determined if different solvents adversely affect the elastic or birefringence properties of gelatin in this type of application. We are presently testing this idea and are testing different gelatin concentrations as well as other photoelastic materials like agarose gels and urethane rubber to determine if the signal stability and photoelastic modulator lifetime can be improved.[27]

ACKNOWLEDGMENTS

The authors thank Marty Johnston for making our Delrin molds and for many useful ideas. They also thank Joe Green and two anonymous reviewers for helpful comments about the manuscript. This work was supported in part by grants from the National Science Foundation (Grant No. 0509869) and the Minnesota Space Grant Consortium.

[a]Present address: 3M Company, 3M Center Building 235-2S-62, St. Paul, MN 55144.
[b]Electronic mail: asgreen@stthomas.edu

[1] S. M. Hauser, L. S. Smith, D. G. Marlowe, and P. R. Yoder, Jr., "The stressed-plate shutter, a new moderate-speed electro-optical light modulator," Appl. Opt. **2**(11), 1172–1175 (1963).
[2] M. Billardon and J. Badoz, "Modulateur de birefringence," C. R. Seances Acad. Sci., Ser. B **262**, 1672–1675 (1966).
[3] L. F. Mollenauer, D. Downie, H. Engstrom, and W. B. Grant, "Stress plate optical modulator for circular dichroism measurements," Appl. Opt. **8**(3), 661–665 (1969).
[4] J. Kemp, "Piezo-optical birefringence modulators: A new use for a long-known effect," J. Opt. Soc. Am. A **59**(8), 950–954 (1969).
[5] PEM-100 photoelastic modulator systems and PEM-100 controller, Hinds Instruments, ⟨www.hindspem.com⟩.
[6] Mark P. Silverman, *Waves and Grains: Reflections on Light and Learning* (Princeton U.P., Princeton, 1998).
[7] J. L. Ferguson, "Two semi-quantitative demonstrations of stress birefringence," Am. J. Phys. **64**(10), 1338–1340 (1996).
[8] T. Oakberg and A. Bryan, "Use of detectors with photoelastic modulators," Proc. SPIE **4819**, 98–106 (2002).
[9] B. Wang, R. R. Rockwell, and A. Leadbetter, "A polarimeter using two photoelastic modulators," Proc. SPIE **5531**, 367–374 (2004).
[10] Detecting the ratio of I_{AC}/I_{AVE}: Measurement of the average intensity of a modulated light beam and Using a mechanical chopper with a PEM to measure V_{DC}, Hinds Instruments, ⟨www.hindspem.com⟩.

[11] ⟨www.pasco.com⟩.
[12] E. Collett, *A Field Guide to Polarization* (SPIE, Bellingham, WA, 2005).
[13] D. Goldstein, *Polarized Light*, 2nd ed. (Marcel Dekker, New York, 2003).
[14] B. Schaefer, E. Collett, R. Smyth, D. Barrett, and B. Fraher, "Measuring the Stokes polarization parameters," Am. J. Phys. **75**(2), 163–168 (2007).
[15] See ⟨www.hindspem.com⟩ for several examples.
[16] T. C. Oakberg, "Measurement of low-level strain birefringence in optical elements using a photoelastic modulator," Proc. SPIE **2873**, 17–20 (1996).
[17] T. C. Oakberg, "Measurement of waveplate retardation using a photoelastic modulator," Proc. SPIE **3121**, 19–22 (1997).
[18] P. D. Hale and G. W. Day, "Stability of birefringent linear retarders (waveplates)," Appl. Opt. **27**(24), 5146–5153 (1988).
[19] The product catalog from Meadowlark Optics, ⟨www.meadowlark.com⟩, illustrates quadratic retardance versus tilt angle curves for various types of wave plates.
[20] B. Wang, "Improved method for measuring low-level linear birefringence in optical materials," Proc. SPIE **3424**, 120–124 (1998).
[21] See for example, ⟨www.newport.com ⟩ or ⟨www.cvilaser.com⟩.
[22] B. Wang, "Measurement of circular and linear birefringence in chiral media and optical materials using the photoelastic modulator," Proc. SPIE **3535**, 294–302 (1998).
[23] M. P. Silverman, W. Strange, J. Badoz, and I. A. Vitkin, "Enhanced optical rotation and diminished depolarization in diffusive scattering from a chiral liquid," Opt. Commun. **132**, 410–416 (1996).
[24] I. A. Vitkin and E. Hoskinson, "Polarization studies in multiply scattering chiral media," Opt. Eng. (Bellingham) **39**(2), 353–362 (2000).
[25] K. C. Hadley and I. A. Vitkin, "Optical rotation and linear and circular depolarization rates in diffusively scattered light from chiral, racemic, and achiral turbid media," J. Biomed. Opt. **7**(3), 291–299 (2002).
[26] A comparison of mechanical and optical properties of water- and ethylene-glycol-based gelatin is given by S. Courty, J. L. Gornall, and E. M. Terentjev, "Mechanically induced helix-coil transition in biopolymer networks," Biophys. J. **90**, 1019–1027 (2006).
[27] A. A. Caputo, E. W. Collard, and J. P. Standlee, "Stresses exhibited in a hydrocolloid under load," J. Dent. Res. **51**(4), 943–949 (1972) discuss the use of agarose gels and urethane rubber for photoelastic analyses in dentistry.

Willyoung Mechanical Pump. Normally this picture series is about apparatus, and here is a splendid example of a mechanical vacuum pump purchased for the use of the students at St. Mary's College in Notre Dame, Indiana. Now the emphasis is on the maker. Elmer Willyoung was a manufacturer of apparatus for electrical measurements (primarily) who worked in Philadelphia in the 1890s. In 1898 he sold his business to his friend, Morris E. Leeds of Philadelphia, who continued to make similar apparatus. In 1903 Leeds joined Edwin Northrup to form Leeds & Northrup, one of the premier makers of electrical measurements apparatus for the first half of the 20th century. I have seen only eleven pieces of Willyoung apparatus in the United States. Information about the maker would be appreciated. (Photograph and Notes by Thomas B. Greenslade, Jr., Kenyon College)